
Synthesis and Characterization of Novel MXeneCeria Heterostructure by Integration of $Ti_3C_2T_x$ Quantum Dots into Fluorescent Nano-octahedral CeO_2

Alireza Rafieerad^{1,2}, Soofia Khanahmadi² and Sanjiv Dhingra^{1,*}

¹*Institute of Cardiovascular Sciences, St. Boniface Hospital Albrechtsen Research Centre, Department of Physiology and Pathophysiology, Max Rady College of Medicine, Rady Faculty of Health Sciences, Biomedical Engineering Program, University of Manitoba, Winnipeg, Manitoba R2H 2A6, Canada*

²*Institute for Molecular Biosciences, Johann Wolfgang Goethe University Frankfurt am Main, 60438, Frankfurt, Germany*

E-mail: sdhingra@sbr.ca; sanjiv.dhingra@umanitoba.ca

**Corresponding Author*

Received 05 September 2024; Accepted 07 January 2025

Abstract

Herein, we report the synthesis of a new stable zero/one-dimensional composite heterostructure “MXeneCeria” by integrating titanium carbide MXene ($Ti_3C_2T_x$) nanosheets-derived quantum dots with nano-octahedral particles of ceria (CeO_2). This unique assimilation resulted in the formation of an auto-fluorescent aqueous colloidal material, which is detectable in fluorescent colors across various wavelengths, ranging from blue to green and red. The unique physicochemical properties of MXeneCeria make it a very promising nanocomposite and it may open a gateway to its potential applications in the biomedical field including tracking, immunoengineering, cell therapy, and targeted drug delivery.

Keywords: $Ti_3C_2T_x$ - CeO_2 , stable nanocolloids, autofluorescent, surface titanium oxides, 0D/1D biomaterial.

International Journal of Translational Science, Vol. 1, 351–362.

doi: 10.13052/ijts2246-8765.2024.004

© 2025 River Publishers

1 Introduction

In recent years, the intersection of nanomedicine and tissue engineering has witnessed significant progress in synthetic bio-nanomaterials and their role in tackling longstanding healthcare challenges [1, 2]. This progress encompasses diverse immunoengineering applications ranging from immunotherapy and cancer theranostics to tissue regeneration [3, 4]. In this regard, low-dimensional MXene materials are considered among the most promising candidates due to their tunable physicochemical, biological, and immunological properties [5, 6]. In particular, MXene nanosheets and derived-quantum dots of specific chemical compositions have been shown to possess competitive immunomodulatory properties [7]. We recently reported the unique immune-regulatory role of MXene quantum dots to treat/alleviate allograft vasculopathy, which is known as an inflammatory disease caused by the host immune responses post-transplantation [8]. These findings and other relevant studies in the literature have significantly broadened the scope of MXenes for biomedical applications. Interestingly, the outcome of recent studies suggests that MXenes with reduced particle sizes and dimensions display enhanced bioactivities due to their ability to enter into the cells and other biological environments [6, 9]. In addition, MXene quantum dots have shown excellent biocompatibility at controlled doses, which might be attributed to their higher aqueous dispersibility with a lower agglomeration tendency and the promise of causing negligible physical damage upon contact with the cells and tissues.

On the other hand, the nanostructures of cerium oxide (nanoceria) are also reported to possess intrinsic immunomodulatory properties, including their potential as anti-cancer agents and defense system against pathogens [10]. Recently significant efforts have been made to combine two or more biomaterials to synthesize a product that captures the best of all the materials used to prepare this new heterostructure. This phenomenon has helped to take the field forward in terms of producing highly efficient user-friendly end products for biomedical applications. In the current study, for the first time, we integrated zero-dimensional $\text{Ti}_3\text{C}_2\text{T}_x$ MXene quantum dots with nano-octahedral particles of ceria to synthesize a novel composite heterostructure – MXeneCerium. Our results suggest that the newly borne MXeneCerium could offer the advantages of MXene quantum dots and nanoceria, and the end product is highly stable zero/one-dimensional material with abundant bioactive surface terminals, including oxygen, hydroxide, and fluorine-containing functional groups.

2 Materials and Methods

2.1 Synthesis of $Ti_3C_2T_x$ MXene Quantum Dots

Commercially available $Ti_3C_2T_x$ flakes (Laizhou Kai Kai Ceramic Materials, Ltd. China) were dispersed in ultrapure water and treated in bath-ultrasonic for ~ 60 min to obtain a colloidal suspension of mono, oligo, and multi-layered $Ti_3C_2T_x$ nanosheets. The $Ti_3C_2T_x$ nanosheets were subjected to homogenization for 30 min. The solutions were transferred into a 100 mL Teflon-lined hydrothermal autoclave reactor and treated overnight at $180^\circ C$. The obtained suspension of MXene quantum dots was then subjected to autoclave sterilization at $121^\circ C$ for 30 min, and the stock solution was stored at $4^\circ C$ for characterization and further experiments.

2.2 Synthesis of Nano-octahedral Particles of Ceria (CeO_2)

The CeO_2 nanoparticles were synthesized by following a previously published protocol [1]. Briefly, commercially available powder of pure cerium nitrate hexahydrate (Sigma-Aldrich) was dispersed in ultrapure water at a concentration of ~ 50 mM. The resultant solution was subjected to hydrothermal treatment in a steel-Teflon autoclave reactor at $\sim 180^\circ C$ for 20–24 hours, followed by centrifugation at 4500 rpm. The obtained colloidal solution of nanoceria was rinsed with pure water to obtain a highly pure colloidal suspension CeO_2 nanoparticles. The final solution was stored at $4^\circ C$ for characterization and further experiments.

2.3 Synthesis of MXeneCerium

The aqueous solutions of $Ti_3C_2T_x$ MXene quantum dots and CeO_2 nanoparticles were mixed at a ratio of 1:1 and stirred overnight at room temperature. The resultant colloidal mixture was centrifuged at 4500 rpm for 30–60 min, the supernatants were then removed to separate the unbound components. The obtained MXeneCerium particles in the precipitate were suspended in ultrapure water and stored at $4^\circ C$ for further experiments.

2.4 Physicochemical Characterization of MXeneCerium

The morphology and microstructure of MXeneCerium was comprehensively characterized using transmission electron microscope attached with an energy-dispersive X-ray spectroscopy detector (FEI Talos, F200X S/TEM, ThermoFisher Scientific), scanning electron microscopy (FEI Nova,

NanoSEM 450 ThermoFisher Scientific), X-ray photoelectron spectroscopy (Kratos Axis Ultra), and Fourier-transform infrared spectroscopy (FTIR, Thermo Scientific Nicolet 6700) at the Manitoba Institute of Materials, University of Manitoba. To assess the phase patterns of the powder and drop-dried samples, an X-ray diffraction (XRD) machine was used at the Department of Geology, University of Manitoba. The peaks were collected in the range from 2-theta 5–80° using a continuous scan with the speed rate of 2/3° min⁻¹ and a report interval of 0.03/0.05°.

2.5 Optical Absorption, Fluorescence, and Stability of MXeneCeria

The UV–visible optical absorption measurements and auto-fluorescence properties of MXeneCeria were determined using a Cytation5 Imaging Multi-Mode Reader (BioTek) and a Nikon Ti-2E microscope. Also, the long-term stability of these colloids was performed at 1, 2, and 5 months of synthesis, and was assessed using UV–Vis spectroscopy measurements.

3 Results and Discussions

Figure 1 depicts the schematic synthesis route as well as the morphology, microstructure, and elemental characterization of MXeneCeria. As shown in panel A, the Ti₃C₂T_x MXene nanosheets were converted to quantum dots with surface titanium oxides through bath-sonication and homogenization for ~60 and 30 min, respectively, followed by hydrothermal treatment of the suspensions at 180°C for ~14 hours. Further, these titanium–carbide/oxide quantum dots were integrated into the as-synthesized nano-octahedral particles of CeO₂ (Supplementary Figure S1). The resultant 0D/1D heterostructure showed a unique morphology with high colloidal stability while retaining the main characteristics of parent materials (Supplementary Figures S2 and S3). Panels B and C display the transmission electron microscopy (TEM) of MXeneCeria clusters. As can be seen, these quantum dots are properly distributed into the ceria particles. Our high-resolution TEM image in panel D exhibits the integrated/lateral structure of the particles. The fast Fourier transform and selected-area-electron-diffraction images of MXeneCeria show the crystalline patterns and lattice d-spacing of its components (panels E, F).

Further, we performed a scanning-TEM (STEM) and energy-dispersive X-ray spectroscopy (EDX) area-scan and elemental-mapping analysis to confirm the purity of the material without significant detection of irrelevant chemical compositions (panels G–O). These data suggest a high

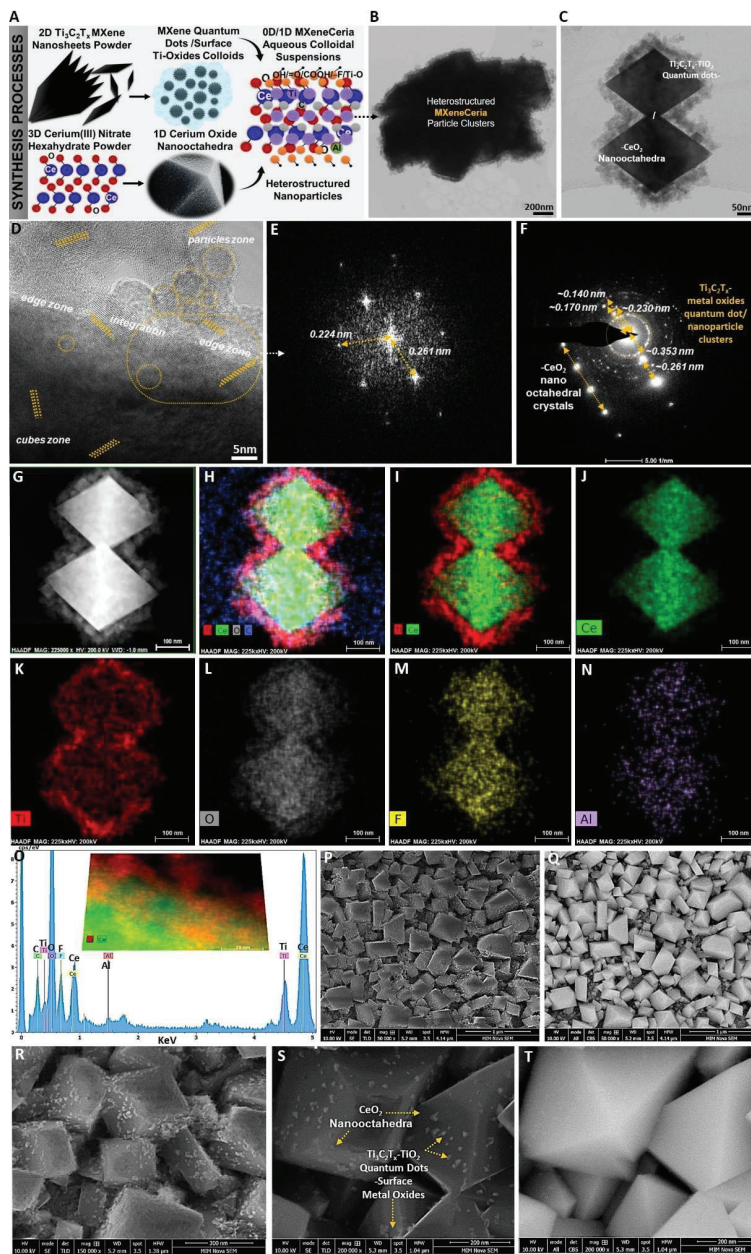


Figure 1 A, The synthesis procedures and B–T, physicochemical morphology and microstructural characterizations of MXeneCerita aqueous colloids.

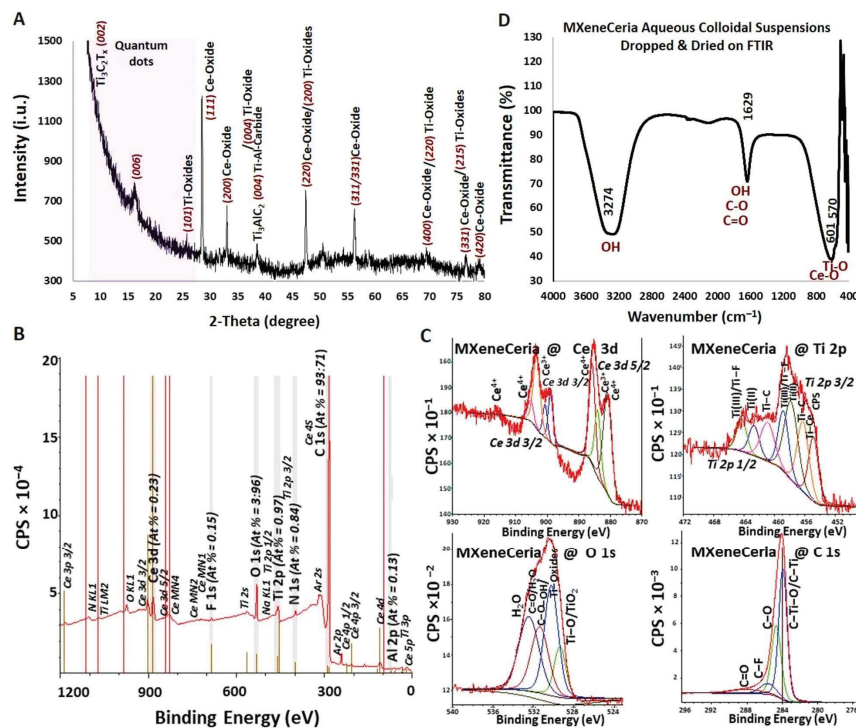


Figure 2 A: The XRD phase pattern. B,C: XPS wide and narrow scan fitting analysis. D: FTIR spectrum of MXeneCeria aqueous colloids.

level of structural integrity alongside typical elemental characteristics of these CeO_2 and $\text{Ti}_3\text{C}_2\text{T}_x$ particles. In addition, panels P–T reveal different magnifications of scanning-EM (SEM) images of these aqueous colloids dried at room temperature. The SEM images captured from the surface of MXeneCeria at secondary-electrons (SE) mode and collective beam scanning (CBS) backscattered electrons illustrate its morphology/surface topography. These data suggest a uniform integration of metal-carbide/oxide particles of $\text{Ti}_3\text{C}_2\text{T}_x$ on the surface of lanthanide oxide ceria nano-octahedra.

We also performed X-ray diffraction and photoelectron spectroscopy (XRD/XPS) to characterize the phase pattern and surface chemistry of MXeneCeria. As shown in panel A of Figure 2, the XRD spectrum of this sample elaborates the detection of primary peaks associated with the chemical compositions of the synthesized composite heterostructure. Also, the XRD phase structure spectra of the raw and parent materials are represented in Supplementary Figure S4. Additionally, as shown in Figure 2B, C,

the XPS survey spectra and narrow scan fitting analysis of the composing elements, including Ce 3d, O 1s, C 1s, and Ti 2p, suggest the successful synthesis and stable chemical bonding between different components of the heterostructured MXeneCerium. The detailed XPS components analysis as well as the corresponding narrow scan fittings of the F 1s, N 1s, and Al 2p are presented in Supplementary Figure S5 and Supplementary Tables S1 to S6. The Fourier transform infrared spectroscopy (FTIR) of this material suggest the presence of organic and/or inorganic components and bonds in its end-structure along with an enrichment of hydroxyl and fluorine-based surface functional groups (Figure 2D). These data align well with other properties of this new material and are in agreement with previous reports in the literature on the physicochemical characterizations of its parent $\text{Ti}_3\text{C}_2\text{T}_x$ MXene and CeO_2 materials.

Furthermore, UV-visible spectroscopy (UV-Vis) was employed to measure the optical absorption and assess the enhanced colloidal dispersibility and stability of MXeneCerium in aqueous media. As demonstrated in Figure 3A–D, Our UV-Vis results suggest the optical absorption property

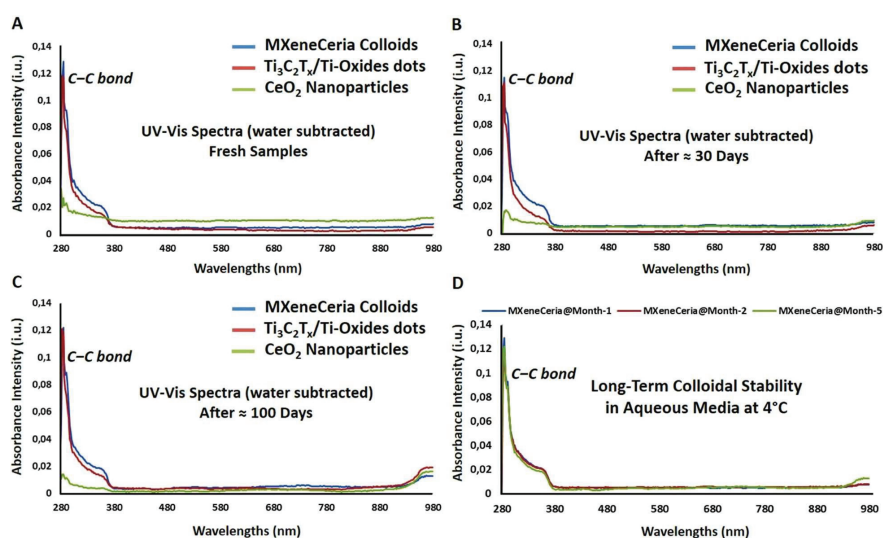


Figure 3 A–D: The UV-visible spectroscopic analysis of pure water, $\text{Ti}_3\text{C}_2\text{T}_x$ MXene nanosheets-derived quantum dots with surface metal oxides, CeO_2 nanoparticles, and MXeneCerium at different wavelengths ranging from 280–980 nm. Data confirm the long-term durability and material stability of these aqueous colloidal suspensions at 4 °C for up to around three months. The MXeneCerium showed no significant changes in the UV-Vis measurement from day 1 to day 100.

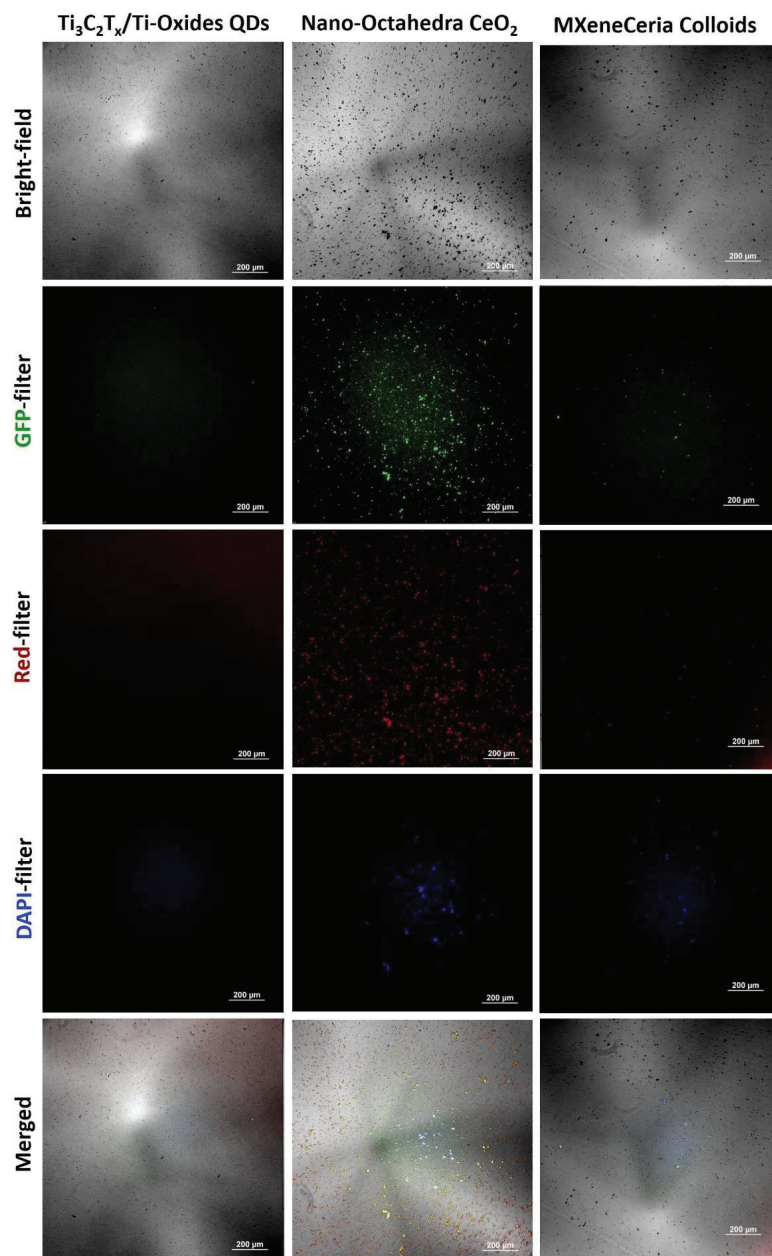


Figure 4 Detection of auto-fluorescence of $Ti_3C_2T_x$ MXene quantum dots with surface metal oxides, CeO_2 nanoparticles, and MXeneCeria composite heterostructure at different wavelengths.

and long-term stability of these collides at 4°C for more than three months (around 100 days). The identification of C–C bonds in the UV–Vis spectra at a wavelength of ~280 nm is a confirmation of the resistance of MXeneCerium against material decomposition in aqueous media.

Lastly, we have evaluated the auto-fluorescent properties of this colloidal material (Figure 4). Interestingly, MXeneCerium has shown fluorescence signals within different tested wavelengths, depicting its potential as a trackable nanoscale biomaterial for various diagnostics and nanomedicine approaches. As can be seen in Supplementary Figure S6, the aqueous colloidal dispersion of MXeneCerium showed relative auto-fluorescent properties, including excitation and emission across different regions and colors. While both of the parent materials used for developing MXeneCerium have been reported to possess high biocompatibility at controlled doses in their nature with intrinsic bioactivity properties for bio-related applications, future detailed studies should focus on investigating the biological/immunological activities and applications of MXeneCerium as well as the mechanisms behind it.

4 Conclusion

In this study, MXeneCerium is fabricated for the first time by integrating $\text{Ti}_3\text{C}_2\text{T}_x$ MXene nanosheet-derived quantum dots into the CeO_2 nano-octahedral particles. This innovative 1D/0D assembly has been found to offer auto-fluorescent properties along with high dispersibility and stability for aqueous colloidal applications. Its microstructure may also benefit from high levels of biocompatibility and bioactivity properties of its parent materials, which is highly advantageous for bio-tracking applications. Another unique aspect of MXeneCerium composite heterostructure lies in the rational formulation of two immunomodulatory biomaterials in a single stable design. Together, these specifications pave the way for future studies.

Acknowledgments

The authors acknowledge research funding from the Natural Sciences and Engineering Research Council of Canada (RGPIN-2021–03951).

Competing Interests

The authors declare no competing interests.

CRediT Authorship Contribution Statement

Alireza Rafieerad: Conceptualization, Methodology, Investigation, Formal Analysis, Validation, Visualization, Writing – Original Draft, Writing – Review & Editing. **Soofia Khanahmadi:** Conceptualization, Formal Analysis, Writing – Original Draft, Writing – Review & Editing. **Sanjiv Dhingra:** Conceptualization, Methodology, Formal Analysis, Validation, Resources, Writing – Original Draft, Writing – Review & Editing.

Data Availability

The data that support the findings of this study are available from the corresponding author upon reasonable request.

References

- [1] Dobrovolskaia, Marina A., and Scott E. McNeil. “Immunological Properties of Engineered Nanomaterials.” *Nature Nanotechnology* 2, no. 8 (2007): 469–78. <https://doi.org/10.1038/nnano.2007.223>.
- [2] Zheng, Yuanyuan, Xiangqian Hong, Jiantao Wang, Longbao Feng, Taojian Fan, Rui Guo, and Han Zhang. “2D Nanomaterials for Tissue Engineering and Regenerative Nanomedicines: Recent Advances and Future Challenges.” *Advanced Healthcare Materials* 10, no. 7 (2021): 2001743. <https://doi.org/10.1002/adhm.202001743>.
- [3] Chuang, Skylar T., Brandon Conklin, Joshua B. Stein, George Pan, and Ki-Bum Lee. “Nanotechnology-enabled immunoengineering approaches to advance therapeutic applications.” *Nano Convergence* 9, no. 1 (2022): 19. <https://doi.org/10.1186/s40580-022-00310-0>.
- [4] Sang, Wei, Zhan Zhang, Yunlu Dai, and Xiaoyuan Chen. “Recent advances in nanomaterial-based synergistic combination cancer immunotherapy.” *Chemical Society Reviews* 48, no. 14 (2019): 3771–3810. <https://doi.org/10.1039/C8CS00896E>.
- [5] Soleymaniha, Mohammadreza, Mohammad-Ali Shahbazi, Ali Reza Rafieerad, Aziz Maleki, and Ahmad Amiri. “Promoting role of MXene nanosheets in biomedical sciences: therapeutic and biosensing innovations.” *Advanced healthcare materials* 8, no. 1 (2019): 1801137. <https://doi.org/10.1002/adhm.201801137>.
- [6] Rafieerad, Alireza, Weiang Yan, Ahmad Amiri, and Sanjiv Dhingra. “Bioactive and trackable MXene quantum dots for subcellular

- nanomedicine applications.” *Materials & Design* 196 (2020): 109091. <https://doi.org/10.1016/j.matdes.2020.109091>.
- [7] Unal, Mehmet Altay, Fatma Bayrakdar, Laura Fusco, Omur Besbinar, Christopher E. Shuck, Süleyman Yalcin, Mine Turktas Erken et al. “2D MXenes with antiviral and immunomodulatory properties: A pilot study against SARS-CoV-2.” *Nano Today* 38 (2021): 101136. <https://doi.org/10.1016/j.nantod.2021.101136>.
- [8] Rafieerad, Alireza, Weiang Yan, Keshav Narayan Alagarsamy, Abhay Srivastava, Niketa Sareen, Rakesh C. Arora, and Sanjiv Dhingra. “Fabrication of smart tantalum carbide MXene quantum dots with intrinsic immunomodulatory properties for treatment of allograft vasculopathy.” *Advanced Functional Materials* 31, no. 46 (2021): 2106786. <https://doi.org/10.1002/adfm.202106786>.
- [9] Arora, Sumit, Jyutika M. Rajwade, and Kishore M. Paknikar. “Nanotoxicology and in vitro studies: the need of the hour.” *Toxicology and applied pharmacology* 258, no. 2 (2012): 151–165. <https://doi.org/10.1016/j.taap.2011.11.010>.
- [10] Ernst, Lena M., and Victor Puentes. “How Does Immunomodulatory Nanoceria Work? ROS and Immunometabolism.” *Frontiers in immunology* 13 (2022): 750175. <https://doi.org/10.3389/fimmu.2022.750175>.

